

Research Article

Cross-Layer Design in Dynamic Spectrum Sharing Systems

A. Shadmand, K. Nehra, and M. Shikh-Bahaei

Department of Electronic Engineering, Division of Engineering, King's College London, WC2R 2LS London, UK

Correspondence should be addressed to K. Nehra, krishna.nehra@kcl.ac.uk

Received 15 January 2010; Revised 28 May 2010; Accepted 9 August 2010

Academic Editor: Hyunggon Park

Copyright © 2010 A. Shadmand et al. This is an open access article distributed under the Creative Commons Attribution License, which permits unrestricted use, distribution, and reproduction in any medium, provided the original work is properly cited.

We consider a dynamic spectrum sharing system consisting of a primary user, whose licensed spectrum is allowed to be accessed by a secondary user as long as it does not violate the prescribed interference limit inflicted on the primary user. Assuming the Nakagami- m block-fading environment, we aim at maximizing the performance of secondary user's link in terms of average spectral efficiency (ASE) and error performance under the specified packet error rate (PER) and average interference limit constraints. To this end, we employ a cross-layer design policy which combines adaptive power and coded discrete M-QAM modulation scheme at the physical layer with a truncated automatic repeat request (ARQ) protocol at the data link layer, and simultaneously satisfies the aforementioned constraints. Numerical results affirm that the secondary link of spectrum sharing system combining ARQ with adaptive modulation and coding (AMC) achieves significant gain in ASE depending on the maximum number of retransmissions initiated by the ARQ protocol. The results further indicate that the ARQ protocol essentially improves the packet loss rate performance of the secondary link.

1. Introduction

The rapidly growing demand for wireless services has led to deployment of the resource allocation approaches that not only provide higher data rates, but also enable the system to guarantee the quality of service (QoS) desired by various services. Cross-layer design has been considered as a promising candidate in this direction. Adaptive modulation and coding (AMC) at the physical layer is widely used to achieve high spectral efficiency (SE) [1–3], but it has to compromise between efficiency and reliability. On the other hand, the automatic repeat request (ARQ) protocol used at the data link layer increases reliability by retransmitting the erroneous packets. The systems exploiting joint design of AMC at the physical layer and ARQ at the data link layer enjoy high throughput with increased reliability as compared to those considering separate implementation of AMC and ARQ [4].

Along with efficiency and reliability, bandwidth is an important concern as the wireless applications become more and more sophisticated and widely used. However, the existing spectrum policies are not competent enough to cope with increasing spectrum access demand, and hence induce

the shortage of available spectrum range. This is due to the fact that the outdated spectrum policies allow little or no sharing, and thus a large part of the useful spectrum remains idle at any given instant and location [5, 6]. The notion of spectrum sharing provides the means of efficient utilization of unused or underutilized parts of spectrum by enabling the unlicensed (secondary) users to exploit licensed (primary) spectrum bands with certain constraints on the interference imposed on licensed users.

Physical layer aspects of spectrum sharing systems have been sincerely studied in literature including [7–9]. The capacity of AWGN channels under received power constraints at the primary receiver for different scenarios, including relay networks, multiple access channels with dependent sources and feedback, and collaborative communication, was analysed in [7]. The authors in [8] derived the capacity and optimum power allocation schemes for different capacity metrics, for example, ergodic, outage, and minimum-rate in Rayleigh fading channels under average and peak received-power constraints at the primary's receiver. Spectrum sharing systems with an additional statistical delay QoS constraint along with the interference-power constraint at the primary receiver were studied in [9].

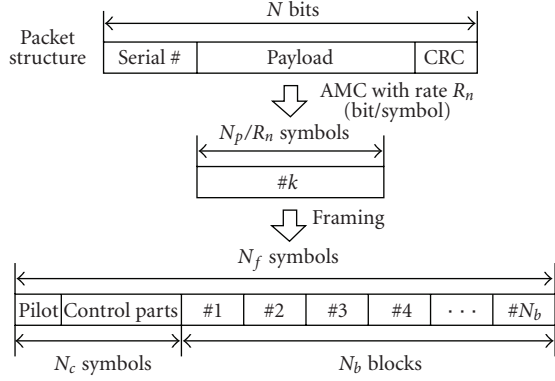


FIGURE 1: Packet and frame structures [4].

The authors determined the maximal possible arrival rate supported by the secondary user's link satisfying aforementioned constraints.

On the other hand, a substantial amount of work has been carried out in the direction of combined AMC-ARQ in the non spectrum-sharing scenario. In [4], a cross-layer design was developed combining constant-power AMC and truncated-ARQ protocol, with the aim of maximizing the spectral efficiency under target delay and packet loss constraints. Joint implementation of variable-power AMC and truncated-ARQ was proposed in [10], and it was demonstrated that combined AMC-ARQ with adaptive power outperforms that with constant-power in terms of ASE as well as packet loss rate. The authors in [11] presented power and rate adaptation policies for coded M-QAM modulation, in order to minimize the packet delay due to queuing at the data link layer, under the prescribed packet error rate constraint.

As per our best knowledge, cross-layer design combining AMC at the physical layer with the ARQ protocol at the data link layer has not been addressed so far in the context of spectrum sharing. In this paper, we study joint design of variable power AMC and truncated-ARQ protocol in the context of spectrum-sharing systems. Our aim is to devise maximum spectral efficiency of the secondary user's link under the constraints of interference-power at the primary receiver, and the target packet error rate.

The remainder of this paper is organized as follows. Section 2 presents the system and channel models, parameters used throughout the paper, and background of the problem addressed. Section 3 deals with the derivation of ASE of the secondary link subject to the specified constraints, and its packet loss probability. Numerical results are discussed in Section 4. Finally, the paper is concluded in Section 5.

2. System Model

Adopting the spectrum-sharing scenario used in [9], we consider a spectrum-sharing system consisting of single primary and secondary users. The secondary user is allowed to operate within the primary user's licensed spectrum, provided that the average interference power inflicted at

the primary receiver does not exceed a certain average threshold. The secondary transmitter employs discrete AMC and power control at the physical layer, and truncated-ARQ protocol at the data link layer. The packets from the secondary's higher layers are stored in an infinite transmit buffer and are grouped into frames for transmission. The secondary transmitter selects an AMC mode, corresponding to a modulation size and forward error correction (FEC) code rate pair [4], and adapts transmit power based on channel state information (CSI) feedback from the secondary and primary receivers. The secondary receiver decodes the received bit streams and places them into a packet structure in order to forward them to the higher layers. Upon erroneous detection of a packet, the ARQ protocol initiates a retransmission and the erroneous packets are selectively retransmitted. The number of retransmissions is bounded by a specific maximum (N_r^{\max}), and the incorrectly received packet after N_r^{\max} transmissions is dropped from the receiver buffer. We adhere to the packet and frame structures shown in Figure 1. The system model has been depicted in Figure 2.

We consider discrete-time block-fading channels for the secondary and primary users' links. The channel gains from the secondary transmitter to the primary and secondary receivers are, respectively, denoted by h^{sp} and h^s . Both h^{sp} and h^s are assumed to be stationary and ergodic with probability density functions (pdf's) $f_{sp}(h^{sp})$ and $f_s(h^s)$, respectively. Furthermore, both h^{sp} and h^s are assumed to be independent and identically distributed (i.i.d.) processes, following the Nakagami- m fading distribution with unit variance. The noise power spectral density and the received signal bandwidth are denoted by N_0 and B , respectively; without loss of generality we assume $N_0B = 1$ for the simplicity of analysis [11]. Moreover, the knowledge of h^{sp} and h^s is assumed to be available at the secondary transmitter. h^s can be fed back from the secondary receiver to the secondary transmitter. h^{sp} can be fed back either directly from the primary receiver to the secondary transmitter or indirectly through a band manager which mediates between two parties [5].

We consider a variable power variable rate transmission scheme at the secondary transmitter, utilizing coded discrete M-QAM modulation. It should be noted that adaptive power and rate of the secondary user are functions of both channel gains h^s and h^{sp} . This is due to average interference power constraint imposed on secondary transmission, defined by

$$\int_{h^s} \int_{h^{sp}} P(h^s, h^{sp}) h^{sp} f_{sp}(h^{sp}) f_s(h^s) dh^{sp} dh^s \leq I_{\max}, \quad (1)$$

where $P(h^s, h^{sp})$ is transmit power of the secondary user, and I_{\max} denotes the maximum allowed interference at the primary receiver. Using the fact that interference constraint (1) depends on the channel gains through the ratio of these parameters [9, (11)], we define a new random variable $v = h^s/h^{sp}$ with the pdf

$$f_v(v) = \frac{\rho^{-m^{sp}}}{\beta(m^{sp}, m^s)} \frac{v^{m^s-1}}{(v + (1/\rho))^{m^{sp}+m^s}}, \quad (2)$$

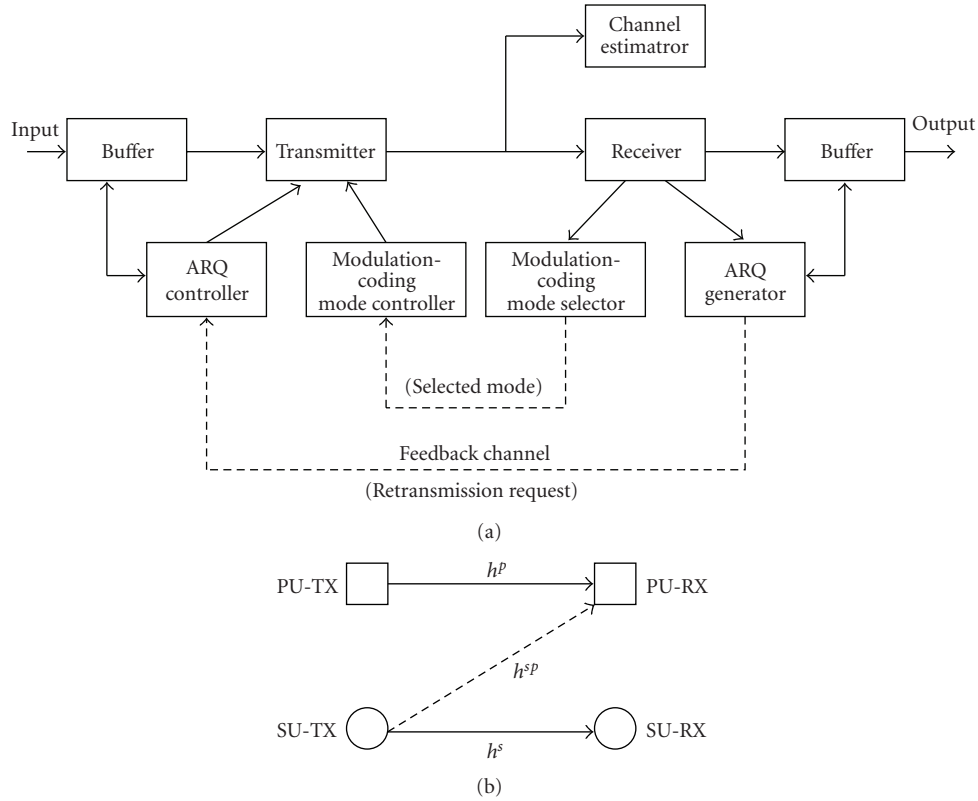


FIGURE 2: System model.

where m^{sP} and m^s denote the Nakagami fading parameters for h^{sP} and h^s , respectively, $\rho = m^s/m^{sP}$, and $\beta(m^{sP}, m^s) = \Gamma(m^{sP})\Gamma(m^s)/\Gamma(m^{sP}+m^s) \cdot \Gamma(\cdot)$ refers to the Gamma function.

Let $\gamma^v = \bar{P}h^{sP}v$ denote the preadaptation secondary received SNR with average secondary transmit power \bar{P} . In order to perform AMC, γ^v is divided into $N + 1$ nonoverlapping consecutive intervals, $[\gamma_n^v, \gamma_{n+1}^v)$, $n = 0, 1, \dots, N$, where $\gamma_0^v = 0$, $\gamma_{N+1}^v = \infty$, and N is the number of AMC modes. The AMC mode n is chosen when $\gamma^v \in [\gamma_n^v, \gamma_{n+1}^v)$, and transmission takes place with rate $R_n(h^s, h^{sP})$ and power $P_n(h^s, h^{sP})$. Both $P(h^s, h^{sP})$ used in (1) and $P_n(h^s, h^{sP})$ are essentially the same, and we will use $P_n(h^s, h^{sP})$ to denote transmit power of the secondary user in rest of the expressions. No transmission occurs when $\gamma^v \in [\gamma_0^v, \gamma_1^v)$, corresponding to the case when h^s is weak compared to h^{sP} . With the purpose of maximizing the spectral efficiency, S_{eff} , of the secondary user, we use the following expression to approximate the secondary channel PER in mode n as a function of postadaptation received SNR, $\gamma^{\text{eq}} = P_n(h^s, h^{sP})h^{sP}v$:

$$\text{PER}_n(\gamma^v) = \begin{cases} 1, & 0 \leq \gamma^v < \gamma_n^{\text{bnd}}, \\ a_n \exp(-g_n P_n(h^s, h^{sP})h^{sP}v), & \gamma_n^{\text{bnd}} \leq \gamma^v. \end{cases} \quad (3)$$

The parameters a_n , g_n , and γ_n^{bnd} are transmission mode and packet-size dependent, and can be obtained by fitting the PER expression given in (3) to the exact PER obtained through simulation. The PER model corresponding to

constant-power allocation at the secondary transmitter has been used and verified in [4].

3. Adaptive Coded Rate and Power Allocation with ARQ

In this section, we deal with the problem of maximizing the spectral efficiency of the secondary user under specified PER and average interference limit constraints. We start with determining the optimal SNR boundaries (v) for AMC mode switching, in order to maximize the ASE under the aforementioned constraints.

3.1. AMC at the Physical Layer. The ASE of the secondary link for discrete AMC case is essentially the sum of data rates of all the modes weighted by the probability of occurrence of the respective mode. Upon selection of the n th mode, each symbol is transmitted with the rate $R_n(h^s, h^{sP}) = R_c \log_2(M_n)$ associated with QAM constellation size M_n and FEC code rate R_c . Presuming a Nyquist pulse shaping filter with bandwidth $B = 1/T_s$, where T_s corresponds to the symbol rate, the ASE achieved at the physical layer without considering possible packet retransmission in the data link layer is expressed by

$$S_{\text{eff}} = \sum_{n=0}^N R_n \Pr(n), \quad (4)$$

where $\Pr(n)$ is the probability of transmission in the n th mode, and is defined by

$$\begin{aligned} \Pr(n) &= \int_{v_n}^{v_{n+1}} f_v(v) dv \\ &= \frac{\rho^{m^s}}{m^s \beta(m^{sP}, m^s)} \left[v^{m^s} {}_2F_1([m^s, m^s + m^{sP}]; [1 + m^s]; -v\rho) \right]_{v_n}^{v_{n+1}}, \end{aligned} \quad (5)$$

where ${}_2F_1([a, b]; [c]; x)$ denotes the Gaussian hypergeometric function [12].

In accordance with the defined random variable v and discrete AMC modes, the average interference constraint given in (1) transforms to

$$\sum_{n=1}^N P_n(h^s, h^{sP}) \int_{v_n}^{v_{n+1}} h^{sP} f_v(v) dv \leq I_{\max}. \quad (6)$$

Using (3), power allocated to the n th mode can be expressed in terms of the PER approximation parameters as

$$P_n(h^s, h^{sP}) = \frac{1}{g_n v h^{sP}} \ln\left(\frac{a_n}{\text{PER}_{\text{ins}}}\right), \quad (7)$$

with (for average transmit power $\bar{P} = 1$, $\gamma^v = v h^{sP}$)

$$\gamma_n^{\text{bnd}} \leq v_n h^{sP} \leq \gamma^v < v_{n+1} h^{sP}, \quad (8)$$

where PER_{ins} represents the achievable instantaneous PER, and

$$\text{PER}_{\text{ins}} \leq P_{\text{tgt}}, \quad \gamma_0^v \leq \gamma^v < \gamma_{N+1}^v, \quad (9)$$

where P_{tgt} denotes the target PER. We formulate the optimization problem of determining the AMC mode switching levels for v , in order to maximize the ASE subject to average interference and instantaneous PER constraints as follows:

$$\begin{aligned} \bar{S}_{\text{eff}} &= \max_{\{v_n\}_{n=1}^N, \text{PER}_{\text{ins}}=0} \sum_{n=1}^N R_n \int_{v_n}^{v_{n+1}} f_n(v) dv \\ \text{s.t. C1: } &\sum_{n=1}^N S_n \int_{v_n}^{v_{n+1}} \frac{1}{v} f_v(v) dv \leq I_{\max} \\ \text{C2: } &\text{PER}_{\text{ins}} \leq P_{\text{tgt}}, \end{aligned} \quad (10)$$

where

$$S_n = \frac{1}{g_n} \log\left(\frac{a_n}{\text{PER}_{\text{ins}}}\right). \quad (11)$$

Constraint C1 represents the maximum allowed interference constraint imposed on the secondary users, and we obtained it by assuming equality in expression (8) and replacing (7) in the average interference constraint equation (6). C2 corresponds to the instantaneous PER constraint. It can be shown that $\sum_{n=0}^N R_n \int_{v_n}^{v_{n+1}} f_v(v) dv$ and the constraints C1 and C2 are convex with respect to v (the proof is given in appendix), and Slater's condition holds, so there is no

duality gap, and the optimal solution is characterized by the Karush-Khun-Tucker conditions [13]. Proof of fulfillment of Slater's condition is provided in Figure 3. X -axis corresponds to right-hand side of the constraint C1, and Y -axis shows the difference between respective LHS and RHS values of the same. Figure 3 ensures that all the values on Y -axis are negative; therefore, there exists v for which strict inequality holds in constraint C1.

To solve the optimization problem (10) for AMC mode switching levels of v , the Lagrangian for this problem is defined as

$$\begin{aligned} L(v_1, v_2, \dots, v_N, \lambda) &= \sum_{n=0}^N R_n \int_{v_n}^{v_{n+1}} f_v(v) dv \\ &+ \lambda \left[\sum_{n=1}^N S_n \int_{v_n}^{v_{n+1}} \frac{1}{v} f_v(v) dv - I_{\max} \right], \end{aligned} \quad (12)$$

where λ is the Lagrangian multiplier. Using the KKT conditions, the optimal solution (v_1, v_2, \dots, v_N) and the corresponding Lagrangian multiplier λ must satisfy the following conditions:

$$\begin{aligned} \frac{\partial L}{\partial v_n^*}(v_1^*, v_2^*, \dots, v_N^*, \lambda^*) &= 0, \quad n = 1, \dots, N, \\ \sum_{n=1}^N S_n \int_{v_n}^{v_{n+1}} \frac{1}{v} f_v(v) dv &= I_{\max}, \\ \text{PER}_{\text{ins}} &\leq P_{\text{tgt}}, \\ \bar{P} h^{sP} v_n^* &> \gamma_n^{\text{bnd}}, \quad n = 1, \dots, N. \end{aligned} \quad (13)$$

Considering (13), the optimal boundary points $\{v_n\}_{n=1}^N$ can be obtained as

$$\begin{aligned} v_1^* &= \frac{\lambda S_1}{R_0 - R_1} = -\frac{\lambda S_1}{R_1}, \quad \text{since } R_0 = 0, \\ v_n^* &= -\frac{\lambda(S_{n-1} - S_n)}{R_{n-1} - R_n}, \quad n = 2, \dots, N. \end{aligned} \quad (14)$$

Value of the Lagrangian multiplier λ can be determined by substituting the boundary points in average interference constraint C1 of (10) with equality sign. We use numerical methods to determine λ . Value of λ corresponds to the boundary points v_n which satisfy the average interference constraint C1 of (10). By using maximum allowed PER limit (P_{tgt}) in (11), λ becomes a function of v , its pdf, and I_{\max} (which also can be fixed to a certain value depending upon the interference level allowed by the primary user). As shown in appendix, the optimization problem (10) is a convex optimization problem; therefore, the boundary points obtained in (14) are also optimal. Substitution of optimal boundary points $v_n, n = 1, \dots, N$ in (4), and (7) yields the optimum ASE and optimum power allocated in n th transmission mode, respectively. Calculation of adaptive power from (7) requires h^{sP} values along with the boundary values of v . Based on our initial assumption of availability of h^{sP} at the secondary transmitter, transmit power in the n th mode can be easily determined.

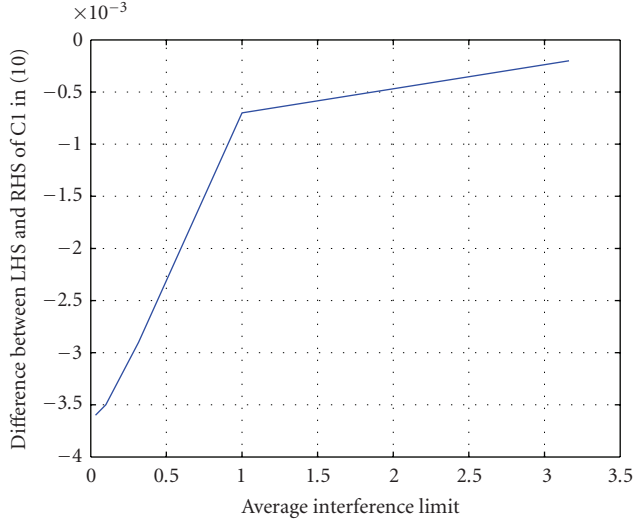


FIGURE 3: Proof of Slater's condition qualification.

3.2. Power Adaptation and AMC Combined with ARQ. Application of the ARQ protocol at the data link layer facilitates retransmission of the erroneous packets received at the secondary receiver. However, for practical purpose, we assume that the number of retransmissions of a packet with error is bounded by a maximum value N_r^{\max} [14, 15]. This is determined by the maximum delay which can be tolerated in communication between the secondary transmitter and the secondary receiver. If a packet is still erroneous after N_r^{\max} retransmissions, it will be dropped from the receiver buffer and will be considered lost. ASE of the secondary link incorporating ARQ can be expressed as

$$\begin{aligned} \bar{S}_{\text{eff}}(N_r^{\max}) &= \frac{\bar{S}_{\text{eff}}}{\bar{N}(\overline{\text{PER}}, N_r^{\max})} \\ &= \frac{\sum_{n=0}^N R_n \Pr(n)}{\bar{N}(\overline{\text{PER}}, N_r^{\max})}, \end{aligned} \quad (15)$$

where $\bar{N}(\overline{\text{PER}}, N_r^{\max})$ is the effective average number of retransmissions per packet (defined in (18)), and $\overline{\text{PER}}$ is the average packet error rate of all modes, and is given by

$$\overline{\text{PER}} = \frac{\sum_{n=1}^N R_n \Pr(n) \overline{\text{PER}}_n}{\sum_{n=1}^N R_n \Pr(n)}. \quad (16)$$

$\overline{\text{PER}}_n$ represents the average PER (the ratio of the number of incorrectly received packets over those transmitted using mode n) in the n th mode, and is defined by

$$\overline{\text{PER}}_n = \frac{1}{\Pr(n)} \int_{v_n}^{v_{n+1}} \text{PER}_n(v) f_v(v) dv. \quad (17)$$

$\bar{N}(\overline{\text{PER}}, N_r^{\max})$ on the secondary link employing joint AMC-ARQ can be determined from the following equation:

$$\bar{N}(\overline{\text{PER}}, N_r^{\max}) = \frac{1 - \overline{\text{PER}}^{N_r^{\max}+1}}{1 - \overline{\text{PER}}}. \quad (18)$$

As described earlier in this subsection, persistence of error in a packet after N_r^{\max} retransmissions results in loss of that packet, and the actual packet loss probability, ϕ_{loss} , for the considered policy is given as

$$\phi_{\text{loss}} = \overline{\text{PER}}^{N_r^{\max}+1} \leq P_{\text{tgt}}^{N_r^{\max}+1} = \Phi_{\text{loss}}, \quad (19)$$

where Φ_{loss} is the maximum acceptable packet loss probability.

3.3. Truncated ARQ without AMC. This section analyzes performance of secondary system employing truncated-ARQ without AMC at the physical layer. Therefore, transmit power and transmission mode are not adaptive to CSI. The average spectral efficiency for the n th transmission mode is calculated with average transmit power \bar{P} . Replacing adaptive power in (3) with \bar{P} , and using (2), the average PER at the physical layer can be obtained as

$$\begin{aligned} \overline{\text{PER}}(n) &= \int_0^{\infty} \text{PER}_n(v) f_v(v) dv \\ &= \int_0^{\gamma_n^{\text{bnd}}} f_v(v) dv \\ &\quad + \int_{\gamma_n^{\text{bnd}}}^{\infty} a_n \exp(-g_n \bar{P} h^{s^p} v) f_v(v) dv \\ &= \frac{\gamma_n^{\text{bnd}}}{1 + \gamma_n^{\text{bnd}}} + \frac{a_n \exp(-g_n \bar{P} h^{s^p} \gamma_n^{\text{bnd}})}{\gamma_n^{\text{bnd}} + 1} \\ &\quad + a_n g_n \bar{P} h^{s^p} \exp(g_n \bar{P} h^{s^p}) \\ &\quad \times Ei(-(\gamma_n^{\text{bnd}} + 1) g_n \bar{P} h^{s^p}) \quad [g_n \bar{P} h^{s^p} > 0], \end{aligned} \quad (20)$$

for $m^s = m^{s^p} = 1$. $Ei(\cdot)$ denotes the exponential integral function. Closed form of average PER at the physical layer for $m^s = m^{s^p} = 2$ can be expressed as

$$\begin{aligned} \overline{\text{PER}}(n) &= \frac{(\gamma_n^{\text{bnd}})^2 (\gamma_n^{\text{bnd}} + 3)}{(\gamma_n^{\text{bnd}} + 1)^3} - \frac{a_n \exp(g_n \bar{P} h^{s^p})}{0.1667} \\ &\quad \times Ei(-g_n \bar{P} h^{s^p} (\gamma_n^{\text{bnd}} + 1)) \\ &\quad \times (g_n \bar{P} h^{s^p})^2 \left(\frac{1}{2} + \frac{g_n \bar{P} h^{s^p}}{6} \right) \\ &\quad + \frac{a_n \exp(-g_n \bar{P} h^{s^p} \gamma_n^{\text{bnd}})}{0.1667 (\gamma_n^{\text{bnd}} + 1)^2} \\ &\quad \times \left(\frac{1}{2} - \frac{g_n \bar{P} h^{s^p} (\gamma_n^{\text{bnd}} + 1)}{2} \right. \\ &\quad \left. - \frac{1}{\gamma_n^{\text{bnd}} + 1} \sum_{k=0}^2 \frac{(-1)^k (g_n \bar{P} h^{s^p})^k (\gamma_n^{\text{bnd}} + 1)^k}{n(n-1) \cdots (n-k)} \right) \\ &\quad [g_n \bar{P} h^{s^p} > 0]. \end{aligned} \quad (21)$$

With N_r^{\max} maximum retransmissions, the average number of transmissions per packet is given by

$$\bar{N}(\overline{\text{PER}}(n), N_r^{\max+1}) = \frac{1 - \overline{\text{PER}}(n)^{N_r^{\max}}}{1 - \overline{\text{PER}}(n)}. \quad (22)$$

Packet loss probability, $\phi_{\text{loss},n}$, and the average spectral efficiency, $\bar{S}_{\text{eff},n}(N_r^{\max})$, can be obtained by the following equations:

$$\phi_{\text{loss},n} = \overline{\text{PER}}(n)^{N_r^{\max+1}},$$

$$\bar{S}_{\text{eff},n}(N_r^{\max}) = \begin{cases} 0 & \bar{P} < \bar{P}_{n,\text{th}} \\ \frac{R_n}{\bar{N}(\overline{\text{PER}}(n), N_r^{\max})} & \bar{P} \geq \bar{P}_{n,\text{th}} \end{cases}, \quad (23)$$

where $\bar{P}_{n,\text{th}}$ is the threshold transmit power beyond which $\phi_{\text{loss},n}$ is guaranteed to be not more than the maximum acceptable packet loss probability, $\phi_{\text{loss},n}$, which may not be true otherwise for nonadaptive systems. It can be identified numerically that the threshold $\bar{P}_{n,\text{th}}$ exists for mode n , which also satisfies interference constraint imposed by primary users. Spectral efficiency of nonadaptive secondary systems employing truncated ARQ has been plotted in Figures 4 and 5.

4. Numerical Results

This section presents numerical results based on the analytical expressions derived in Section 3, to quantify the performance gain of the proposed scheme in terms of overall spectral efficiency and error performance. The analytical expressions have been developed for the Nakagami- m block fading channel links h^s and h^{sp} . However, to generate the numerical results, in this section we consider two specific cases of the Nakagami distribution namely, $m = 1$, which is nothing but the Rayleigh distribution, and $m = 2$. Adopting the PER approximation parameters of six-mode AMC scheme for packet length $N_b = 1080$ from [4, Table 2], we choose the maximum allowed packet error probability for the secondary link as $\Phi_{\text{loss}} = 10^{-3}$. The PER approximation parameters $a_n, g_n, \gamma_n^{\text{bnd}}$ are determined by the AMC mode chosen corresponding to the random variable v , which is the ratio of channels gains. We compare ASE resulting from optimized AMC-ARQ for the secondary link under average interference power constraint, with channel capacity of the corresponding distribution derived in [16].

ASE of the secondary link corresponding to different values of N_r^{\max} is plotted against average inflicted interference limit at the primary receiver in Figures 4 and 5, for $m = 1$ and $m = 2$, respectively. It is apparent from (15) that $N_r^{\max} = 0$ corresponds to the special case of AMC only. Figures 4 and 5 depict that combined AMC-ARQ at the secondary transmitter provides significant gain in spectral efficiency over AMC only, for both fading scenarios. This is due to the underlying error correcting capability of truncated-ARQ, which depends on the maximum number of retransmissions. Error correcting capability of ARQ increases

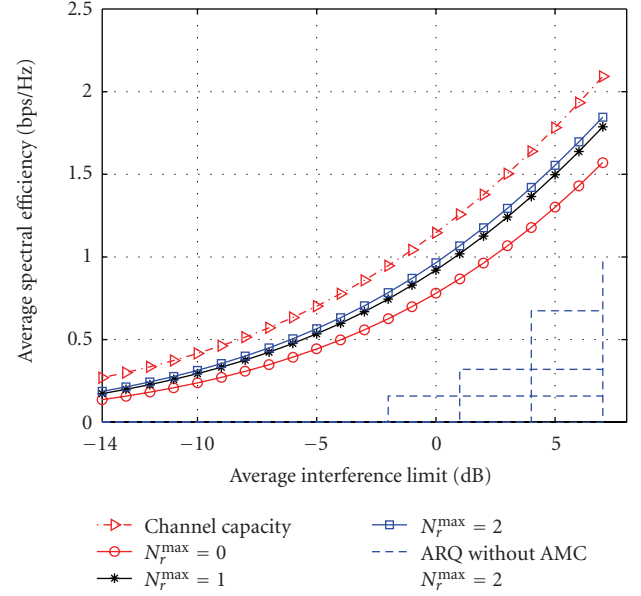


FIGURE 4: Average spectral efficiency versus interference limit for Rayleigh distributed h^s and h^{sp} .

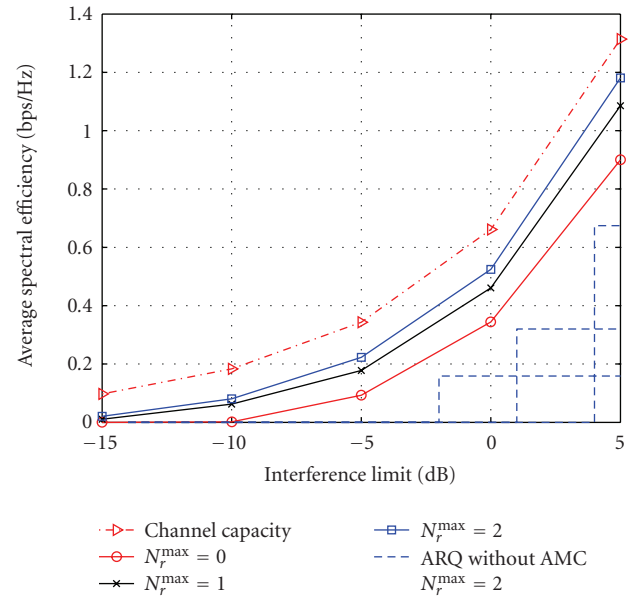


FIGURE 5: Average spectral efficiency versus interference limit for Nakagami distributed ($m = 2$) channel links.

with N_r^{\max} , which benefits physical layer by relaxing the stringent error correction requirements. This lower performance requirement at physical layer is exploited to increase the transmission rates, which results in overall spectral efficiency improvement [4]. Closeness of the spectral efficiency curve corresponding to $N_r^{\max} = 2$ to the respective channel capacity corroborates this. However, increasing N_r^{\max} beyond 2 does not further increase the ASE, which is asserted in Figure 6. Figures 4 and 5 also show the gain in ASE achieved by physical layer optimization, that is, AMC only over

nonadaptive system with truncated ARQ. Figure 6 depicts the effect of N_r^{\max} on ASE of the secondary user in the Rayleigh and the Nakagami distributed scenarios. It can be clearly noticed that the spectral efficiency in both fading scenarios becomes almost constant after $N_r^{\max} = 2$. Figure 6 also indicates that the spectral efficiency of the secondary link following the Rayleigh distribution is greater than that following the Nakagami distribution. This is in contrast to the spectral efficiency of fading channel under transmit power constraint for which the spectral efficiency increases when the Nakagami parameter increases.

Figure 7 demonstrates error performance of the proposed policy by plotting the packet loss probability as a function of target PER, with and without ARQ. It is evident from the plots that application of the ARQ protocol significantly improves error performance of the secondary link, for both the fading scenarios considered. This is in general true for channel links following the Nakagami- m distribution.

5. Conclusion

In this paper, we developed a cross-layer design scheme in a dynamic spectrum sharing system consisting of single primary and secondary users. We considered a spectrum sharing scenario, where the secondary user can operate within the primary user's licensed spectrum, provided that the average interference power inflicted at the primary receiver does not exceed a certain average threshold. The secondary transmitter exploited cross-layer design by employing discrete AMC with adaptive power control at the physical layer, and the truncated-ARQ protocol at the data link layer. We determined AMC mode switching levels of h^s/h^{sp} , in order to maximize the performance of the secondary link in terms of ASE and error performance under the specified packet error rate (PER) and average interference limit constraints. Numerical results verified that the secondary link of the considered system combining ARQ with AMC achieves significant gain in ASE depending on the maximum number of retransmissions initiated by ARQ protocol. The results further lead to the conclusion that increasing the number of retransmissions improves packet loss rate probability performance of the secondary link.

Appendix

In order to prove the convexity of (10), let $\chi(v_1, v_2, \dots, v_N)$ denote the objective function in (10), that is,

$$\chi(v_1, v_2, \dots, v_N) = \sum_{n=0}^N R_n \int_{v_n}^{v_{n+1}} f_v(v) dv, \quad (24)$$

where $f_v(v)$ is given by (2). We introduce the following lemma.

Lemma 1. For a Nakagami- m fading pdf, $v \geq (m^s - 1)/(m^{sp} + 1)\rho$ is a sufficient condition for convexity of both the function χ and constraint function in (10).

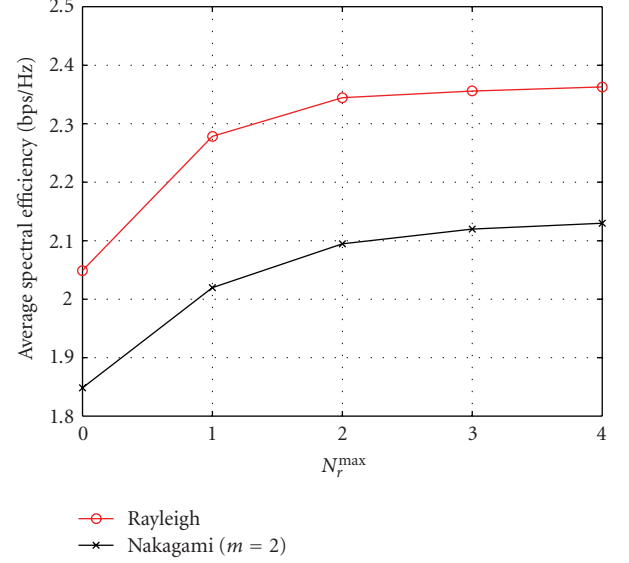


FIGURE 6: Average spectral efficiency versus number of retransmissions, $I_{\max} = 10$ dB.

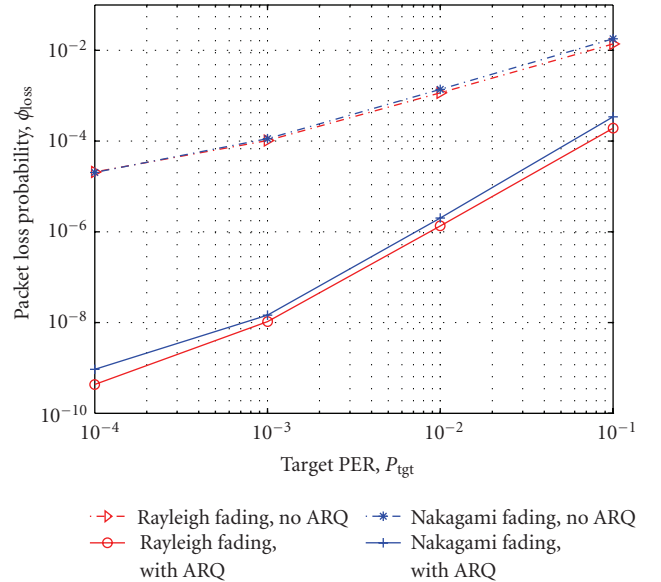


FIGURE 7: Packet loss probability versus the target PER, $I_{\max} = 10$ dB, $N_r^{\max} = 1$.

Proof. First consider the χ function. Since $\partial^2 \chi / \partial v_i \partial v_j = 0$; $i, j, \dots, N, i \neq j$, for χ to be convex, it is sufficient to have $\partial^2 \chi / \partial v_i^2 \geq 0$ [13]. We have

$$\frac{\partial^2 \chi}{\partial v_i^2} = (R_{i-1} - R_i) \frac{\partial f_v(v)}{\partial v} \Big|_{v=v_i}. \quad (25)$$

Since $R_{i-1} < R_i$, in order to guarantee $\partial^2 \chi / \partial v_i^2 \geq 0$, it is required to have $\partial f_v(v) / \partial v \leq 0$, for all i ,

$$\begin{aligned}
\frac{\partial f_v(v)}{\partial v} &= \left(\frac{\rho^{-m^s p}}{\beta(m^s p, m^s)} \right) \\
&\times \left[\frac{((m^s - 1)v^{m^s - 2})}{(v + (1/\rho))^{m^s p + m^s}} \right. \\
&\quad \left. - \frac{((m^s p + m^s)(v + (1/\rho))^{m^s p + m^s - 1} v^{m^s - 1})}{(v + (1/\rho))^{m^s p + m^s}{}^2} \right] \\
&= \left(\frac{\rho^{-m^s p}}{\beta(m^s p, m^s)} \right) \\
&\times \left[\frac{((m^s - 1)v^{m^s - 2})(v + (1/\rho)) - (m^s p + m^s)v^{m^s - 1}}{(v + (1/\rho))^{m^s p + m^s}} \right]. \quad (26)
\end{aligned}$$

Since the denominator of the above fraction is always positive, in order to guarantee $\partial f_v(v)/\partial v \leq 0$, the numerator should be negative. This leads to

$$v \geq \frac{(m^s - 1)}{(m^s p + 1)\rho}, \quad (27)$$

which is satisfied for all AMC modes. Now considering the constraint C1 in (10), denoted by

$$\omega(v_1, v_2, \dots, v_N) = \sum_{n=1}^N S_n \int_{v_n}^{v_{n+1}} \frac{1}{v} f_v(v) dv \leq I_{\max}, \quad (28)$$

where $S_n = g_n \log(a_n/P_{\text{tgt}})$, it is easy to check that $\partial^2 \omega / \partial v_i v_j = 0$; $i, j, \dots, N, i \neq j$, and

$$\frac{\partial^2 \omega}{\partial v_i^2} \geq \frac{(S_i - S_{i-1})}{v_i^2} f_v(v_i) - \frac{(S_i - S_{i-1})}{v_i} \frac{\partial f_v(v)}{\partial v} \Big|_{v=v_i}. \quad (29)$$

Since $S_i > S_{i-1}$, the first term in the R.H.S of (29) is positive. From discussion on convexity of χ function, we know that when $v \geq (m^s - 1)/(m^s p + 1)\rho$, we have $\partial f_v(v)/\partial v \leq 0$, and therefore, the second term in R.H.S of (29) is also positive and consequently $\partial^2 \omega / \partial v_i^2 \geq 0$, and hence ω function is convex. \square

References

- [1] M. Shikh-Bahaei, "Joint optimization of "transmission rate" and "outer-loop SNR target" adaptation over fading channels," *IEEE Transactions on Communications*, vol. 55, no. 3, pp. 398–403, 2007.
- [2] D. Niyato and E. Hossain, "Competitive spectrum sharing in cognitive radio networks: a dynamic game approach," *IEEE Transactions on Wireless Communications*, vol. 7, no. 7, pp. 2651–2660, 2008.
- [3] S. Sampei and H. Harada, "System design issues and performance evaluations for adaptive modulation in new wireless access systems," *Proceedings of the IEEE*, vol. 95, no. 12, pp. 2456–2471, 2007.
- [4] Q. Liu, S. Zhou, and G. B. Giannakis, "Cross-layer combining of adaptive modulation and coding with truncated ARQ over wireless links," *IEEE Transactions on Wireless Communications*, vol. 3, no. 5, pp. 1746–1755, 2004.
- [5] J. M. Peha, "Approaches to spectrum sharing," *IEEE Communications Magazine*, vol. 43, no. 2, pp. 10–12, 2005.
- [6] T. A. Weiss and F. K. Jondral, "Spectrum pooling: an innovative strategy for the enhancement of spectrum efficiency," *IEEE Communications Magazine*, vol. 42, no. 3, pp. S8–S14, 2004.
- [7] M. Gastpar, "On capacity under received-signal constraints," in *Proceedings of the 42nd Annual Allerton Conference on Communication, Control and Computing*, Citeseer, 2004.
- [8] L. Musavian and S. Aïssa, "Capacity and power allocation for spectrum-sharing communications in fading channels," *IEEE Transactions on Wireless Communications*, vol. 8, no. 1, pp. 148–156, 2009.
- [9] L. Musavian and S. Aïssa, "Adaptive modulation in spectrum-sharing systems with delay constraints," in *Proceedings of the IEEE International Conference on Communications (ICC '09)*, pp. 1–5, June 2009.
- [10] J. S. Harsini and F. Lahouti, "Joint optimization of adaptive modulation and coding, power control and packet retransmission over block fading channels," in *Proceedings of the IEEE Information Theory Workshop on Information Theory for Wireless Networks (ITW '07)*, pp. 1–5, July 2007.
- [11] J. S. Harsini and F. Lahouti, "Adaptive transmission policy design for delay-sensitive and bursty packet traffic over wireless fading channels," *IEEE Transactions on Wireless Communications*, vol. 8, no. 2, pp. 776–786, 2009.
- [12] I. Gel'fand, S. Gindikin, and M. Graev, *Selected Topics in Integral Geometry*, Amer Mathematical Society, 2003.
- [13] S. Boyd and L. Vandenberghe, *Convex Optimization*, Cambridge University Press, New York, NY, USA, 2004.
- [14] A. Shadmand and M. Shikh-Bahaei, "Tcp dynamics and adaptive mac retry-limit aware link-layer adaptation over ieee 802.11 wlan," in *Proceedings of the 7th Annual Conference on Communication Networks and Services Research (CNSR '09)*, pp. 193–200, May 2009.
- [15] Q. Li and M. van der Schaar, "Providing adaptive qos to layered video over wireless local area networks through real-time retry limit adaptation," *IEEE Transactions on Multimedia*, vol. 6, no. 2, pp. 278–290, 2004.
- [16] A. Ghasemi and E. S. Sousa, "Capacity of fading channels under spectrum-sharing constraints," in *Proceedings of the IEEE International Conference on Communications (ICC '06)*, vol. 10, pp. 4373–4378, July 2006.